*Science & Global Security, 18:87–118, 2010*

*ISSN: 0892-9882 print / 1547-7800 online*
*DOI: 10.1080/08929882.2010.493078*

Routledge
Taylor & Francis Group

# Analysis of Debris from the Collision of the Cosmos 2251 and the Iridium 33 Satellites

Ting Wang

Peace Studies Program, Cornell University, Ithaca, New York, USA

The collision between the active American Iridium 33 satellite and the retired Russian Cosmos 2251 satellite on 10 February 2009, is the first on-orbit collision between satellites. As of 1 December 2009, the U.S. space tracking system catalogued 1,632 fragments from the collision, many of which will stay in orbit for decades. This paper estimates the total number, size, area-to-mass ratio, and relative velocity of the catalogued fragments; calculates the lifetime and orbital evolution of the fragments; and evaluates the short- and long-term hazards they pose in the space environment. It is shown that previous estimates of the probability that an intact object in space will collide with another object appear to be lower than is indicated by observed collisions. How the collision probability depends on the shapes of the colliding objects is analyzed, and results indicate that including shape dependence will increase estimates of collision probability. Previous analyses have not considered the effects of satellites appendages, which lead to an underestimation of the long-term space debris population.

## INTRODUCTION

The collision on 10 February 2009 between the Iridium 33 satellite and the defunct Cosmos 2251 satellite at an altitude of 770 km (470 miles) is the first known collision of two intact satellites.

The Iridium satellite was part of a constellation of communication satellites owned by Iridium Satellite LLC, a privately held U.S. company based in Bethesda, Maryland. The dry mass of the satellite was 556 kg. The Cosmos satellite, which had a dry mass of 900 kg, was owned by Russia. It was launched in 1993 and is not believed to have been active or capable of maneuvering at the time of the collision.

Received 9 March 2010; accepted 3 May 2010.
Address correspondence to Ting Wang, 152 Uris Hall, Cornell University, Ithaca, NY 14853, USA. E-mail: mr.wangting@gmail.com.

The two satellites were both orbiting the Earth at a speed of nearly 7.5 km/s, and collided at a speed well over 10 km/s. The collision produced space debris ranging in size from large, massive pieces to dust particles. The debris cloud poses a hazard to nearby satellites.

This paper uses data published by the U.S. Space Surveillance Network (SSN) and estimates based on the NASA Standard Breakup Model[1] to calculate the number, size, area-to-mass ratio, and relative velocity of the fragments produced by the collision. It uses this information to determine the orbital lifetime and orbital evolution of the fragments, and to assess the effects of this collision on the space environment.

## FRAGMENT PARAMETERS

The parameters used to characterize fragments include average size, mass, area-to-mass ratio (the cross-sectional area of the fragment divided by its mass), and relative velocity (the fragment velocity immediately after the breakup relative to the satellite's center-of-mass). These parameters serve as inputs for calculating the fragments' orbital evolution and assessing their effects on the space environment.

This paper uses observational data from the U.S. Space Surveillance Network on the collision fragments to estimate these parameters.

These results are compared to those predicted by the NASA Standard Breakup Model, which is an empirical model based on historical breakup events and ground tests. The model gives estimates of distributions of fragment parameters based on the collision velocity and mass of the colliding objects. Not surprisingly, these estimates can differ significantly from the observed results for specific breakup events. For example, the model underestimated the number of fragments from the destruction of the Chinese Fengyun satellite in January 2007 by a factor of three.[2,3]

### Number and Size of the Iridium-Cosmos Fragments

The United States maintains a "catalog" of objects in space. To be in the catalog, an object must be tracked by the SSN and its origin must be known. As a result, it is possible to identify the entries in the catalog that correspond to the observed fragments from the two satellites. Currently the catalog contains some 15,000 objects, as well as a few thousand additional objects that are tracked by the SSN but whose origin is not known. The observational data is published in the form of "two-line elements" (TLEs), which specify an object's orbit at a given time.[4]

SSN typically can track objects in LEO with size larger than about 10 cm. Since the SSN is still detecting and cataloging fragments from the collision,

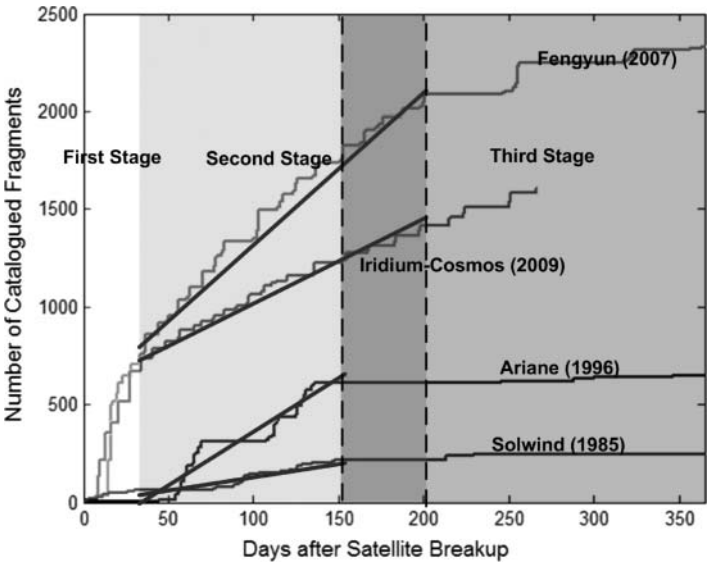


**Figure 1:** Number of SSN catalogued fragments with time for four satellite breakups.

a total number of fragments is probably larger than the currently observed. Therefore, to predict the actual number of large fragments, the observation histories of past breakups are investigated. Figure 1 shows the SSN fragment cataloging process of the Iridium-Cosmos collision and three past events in low Earth orbit (LEO, below 2,000 km altitude).[5] The plot shows that the cataloging process of LEO objects can be divided into three stages. After the first month (stage 1), the SSN finds and tracks fragments at a stable rate for the next 4 to 6 months. Stage 2 typically starts at 30 days after the breakup and ends at 150–200 days after the breakup. Most of the fragments are cataloged during this period. In stage 3, the SSN occasionally finds additional fragments. This stage typically continues for several years. Roughly 2 to 25% of fragments are found during this stage.

As can be seen from Figure 1, the second stage for the Iridium-Cosmos collision ends at roughly 200 days after breakup. Assuming that 25% more fragments could be found during the third stage, the current and estimated catalogued numbers from the Iridium 33 and Cosmos 2251 satellites are given in Table 1.

Although adding the Cobra Dane radar in 2003 allowed the SSN to track fragments with size as small as 5 cm,[6] debris particles with size between 5 cm and 10 cm only account for 3% of all catalogued objects.[7] Since the SSN could also miss fragments larger than 10 cm,[8] the number of cataloged fragments is assumed to be equal to the number of fragments with size greater than 10 cm, as a conservative estimate.

**Table 1:** Number of catalogued fragments from the Iridium and Cosmos satellites

| | Cosmos 2251 | Iridium 33 | Sum |
|---|---|---|---|
| Number of catalogued fragments (12/1/09) | 1,142 | 490 | 1,632 |
| Estimated total number larger than 10 cm | 1,300 | 550 | 1,850 |

As a comparison, Table 2 shows the number of fragments of various sizes resulting from the Iridium-Cosmos collision as calculated from the NASA Breakup Model using the dry masses of the satellites. As noted above, the SSN can typically track objects in LEO with size larger than about 10 cm, so the first column of fragment numbers in Table 2 is relevant for comparing to observations.

The physical size of each cataloged fragment can be estimated from the SSN data. That data includes the observed Radar Cross Section (RCS) of most of the cataloged fragments, which is a measure of the reflected radar signal from each object. The NASA Size Estimation Model (SEM) can then be used to convert the RCS to an average size for each object.[9]

Figure 2 shows the cumulative size distributions of the Iridium and Cosmos fragment clouds, that is, the number of fragments larger than a given size, using the observed data and SEM. In going to smaller sizes, the curves of observed data level off below about 10 cm due to lack of sensitivity of the SSN radars.

The data in Figure 2 roughly follow a power-law distribution, which is consistent with the functional form assumed in the NASA Breakup Model. However, the parameters of the fitted curves differ from those of the NASA model curves. If the power law is correct, the number of Cosmos fragments greater than 1 cm will be more than twice as large as that estimated by NASA model. The number of Iridium fragments larger than 10 cm is close to the NASA model's estimation (see Table 1). Similarly, the NASA model predicts significantly more fragments larger than 1 m in both cases than is actually seen.

**Table 2:** Numbers of fragments of various sizes estimated using the NASA Breakup Model

| | >10 cm | >1 cm | >1 mm |
|---|---|---|---|
| Cosmos 2251 | 840 | 43,220 | 2.22 e6 |
| Iridium 33 | 580 | 30,100 | 1.54 e6 |
| Sum | 1,420 | 73,320 | 3.76 e6 |

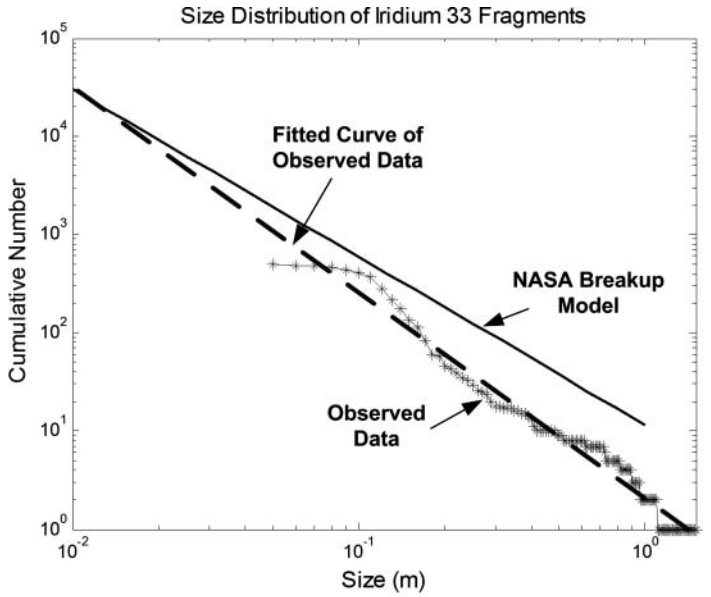


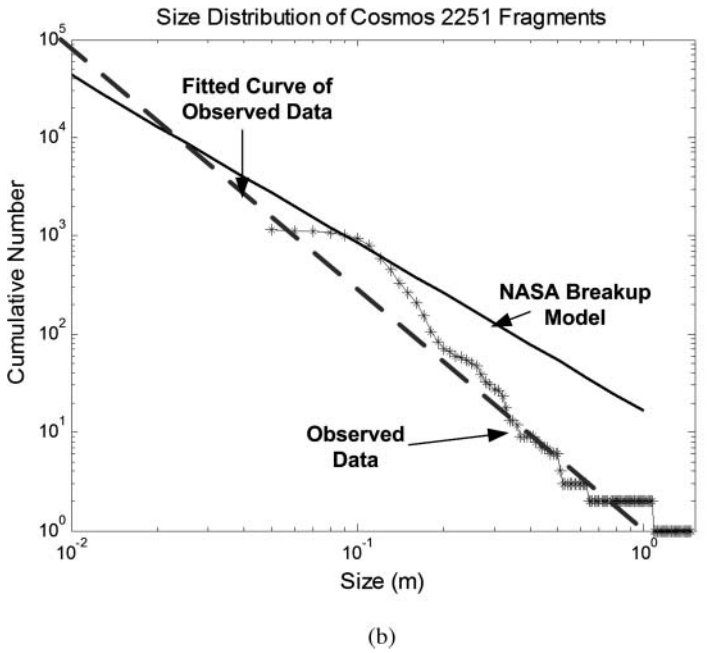


**Figure 2:** Cumulative size distributions of Iridium and Cosmos fragment clouds. The curves show the number of fragments larger than a given size, where the size is determined by using NASA's SEM model to convert radar cross section into physical size. In going to smaller sizes, the curves of observed data level off below about 10 cm due to lack of sensitivity of the SSN radars. These plots show that the data appears to follow a power law, but with different parameters than predicted by the NASA Breakup Model. (a) Iridium 33; (b) Cosmos 2251.

## Area-to-Mass Ratio of the Iridium-Cosmos Fragments

The orbital lifetime of fragments is related to their area-to-mass ratio (A/M). The observed change in the semi-major axis of a fragment's orbit over time, which can be determined from the published history of TLEs, can be related to the change in the fragment's energy. By considering the perturbations on the orbit, such as solar pressure, one can isolate the effect due to atmospheric drag and calculate the mechanical work done by atmospheric drag acting upon the object. The energy loss depends on A/M and the atmospheric density. By using a detailed atmosphere model, one can therefore estimate A/M for each fragment. The actual algorithm applied numerical filtering technology to remove effects caused by other perturbations.[10] The algorithm used for this paper uses the NRLMSIS 00 atmosphere model[11] and the actual daily solar flux record. TLEs up to 31 October 2009 are used to calculate the results.

Figure 3 shows the distribution of A/M of the catalogued fragments from the two satellites. The A/M ratios of most Iridium fragments are greater than those of Cosmos, which will result in a shorter lifetime for the Iridium fragments. Other researchers have used different methods but found a similar A/M distribution.[12]

As is shown in Figure 4, Iridium has three large solar panels, while the solar cells of Cosmos are attached to its body. The fragments with higher A/M are

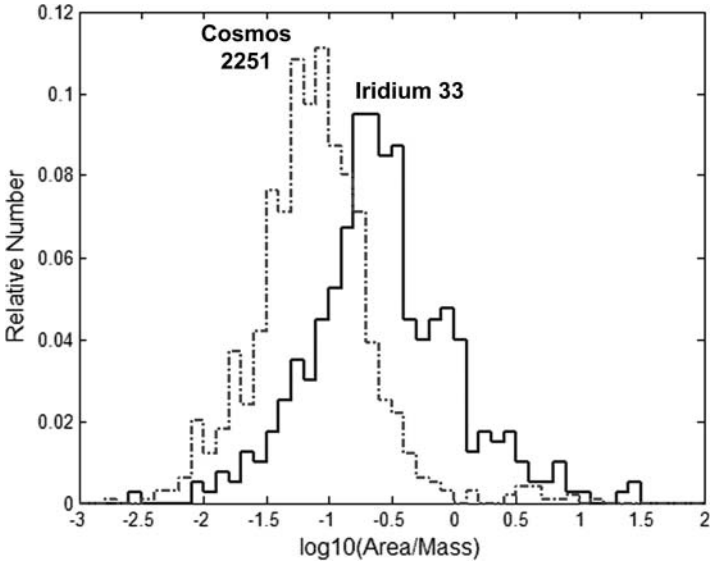


**Figure 3:** The area-to-mass ratio (A/M) of the catalogued fragments from the Iridium and Cosmos satellites.

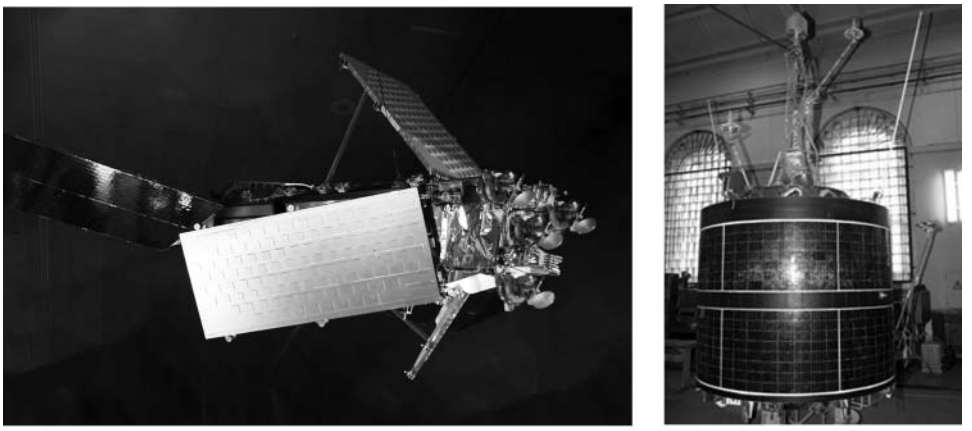

(a) (b)

**Figure 4:** Images of the Iridium and Cosmos satellites. (a) Iridium 33; (b) Cosmos 2251.

likely from materials in the solar panels of the Iridium. A similar phenomenon was observed in the Chinese Fengyun breakup.

## Mass of the Iridium-Cosmos Fragments

The mass of the fragments can be estimated from the parameters calculated above, since the mass of a fragment should be proportional to the square of its characteristic size divided by its area-to-mass ratio.

In particular, the mass of a specific catalogued fragment $m_i$ can then be estimated by

$$m_i = \frac{\alpha l_i^2}{(A/m)_i} \tag{1}$$

$$\alpha = \frac{\beta M}{\sum_{i=1}^{N} \frac{l_i^2}{(A/m)_i}}$$

where $l_i$ is the average size of the fragment

$(A/m)_i$ is the area-to-mass ratio of the fragment

$M$ is the mass of the satellite

$N$ is the number of catalogued fragments from the breakup of the satellite

$\beta$ is the ratio between the total mass of the detected fragments and mass of the satellite, which can be assumed to be 0.7–0.95.

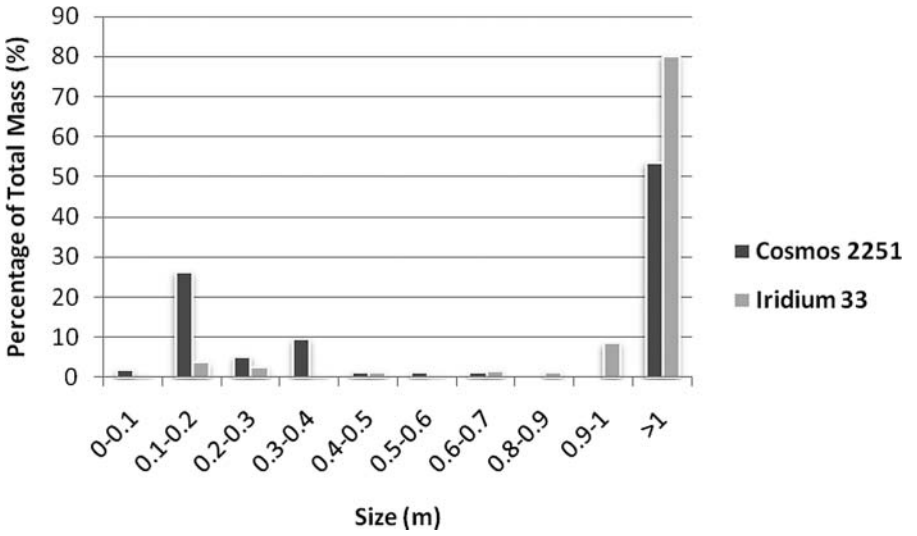


**Figure 5:** Distribution of the mass of catalogued collision fragments with size. For both satellites, the bars show the total mass of fragments in each size range, relative to the total mass of the original satellite.

The coefficient $\alpha$ is included to ensure that the sum of the masses of all $N$ fragments equals $\beta M$, which is the mass of the original satellite carried away in the cataloged fragments.

The error in the calculated mass for a specific fragment is probably large since the value of the RCS, the conversion of RCS to physical size, and the calculated values of A/M are all uncertain. Moreover, the mass of undetected fragments is not known. However, since these uncertainties affect all of the fragments, the relative mass distribution of the fragments should be fairly accurate. Figure 5 shows how the total mass of catalogued fragments of a given size varies with size for the two satellites.

According to Figure 5, roughly 80% of the mass of the Iridium satellite is concentrated in several massive fragments. Calculations show that the largest fragment of Iridium might contain more than half of the total mass. The SSN catalog assigns this large fragment the ID number 24946, which was the number assigned to the original Iridium 33.

Similarly, more than half of the mass of the Cosmos satellite is contained in a few large pieces. Since the bulk of Iridium and much of Cosmos appear to be intact, the collision appears not to have been a head-on collision between the bodies of the two satellites.

Compared to Iridium, a greater fraction of the mass of Cosmos broke into smaller fragments, with more than 25% of the total mass of Cosmos concentrated in fragments with size from 10 cm to 20 cm. Smaller, untrackable fragments may comprise more than 20% of the satellite mass. The reason for this

difference might be that Cosmos is more compact than Iridium so that the energy from the collision was more strongly coupled to the body of the satellite.

## Relative Velocity of the Iridium-Cosmos Fragments

In a satellite breakup, each fragment gains energy and momentum, which gives it a relative velocity with respect to the parent satellite. The method used to determine the relative velocity of the fragments from the observed TLEs is described in Appendix A.

The relative velocity distribution of the cataloged fragments from the collision is shown in Figure 6. The distribution for Cosmos fragments is shifted to higher speeds than that of the Iridium fragments. This result is contrary to the NASA Breakup Model, which estimates that fragments with higher A/M will have higher relative speed (see Figure 7), while the distribution of A/M for the Cosmos fragments is centered at a lower value than the Iridium fragments.

The data in Figure 7 show that in this collision, the Fengyun breakup, and the 1985 SOLWIND breakup the relationship between A/M and relative speed of the catalogued fragments differs significantly from the predictions of the NASA model. The NASA model predicts a power-law relation between the A/M and the mean speed of fragments with that value of A/M, while the data show a much different functional form. In particular, the mean speed appears to be relatively constant when A/M is between 0.01 and 1. These events indicate

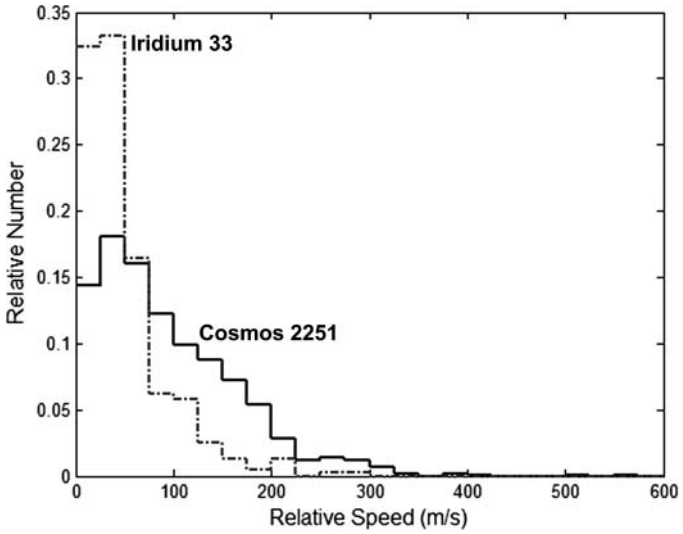


**Figure 6:** Distribution of relative speed of the catalogued fragments from the Iridium and Cosmos satellites. Since the original speed of the satellites is about 7.5 km/s, the relative speed of the vast majority of the fragments is only a couple percent of their orbital speed.

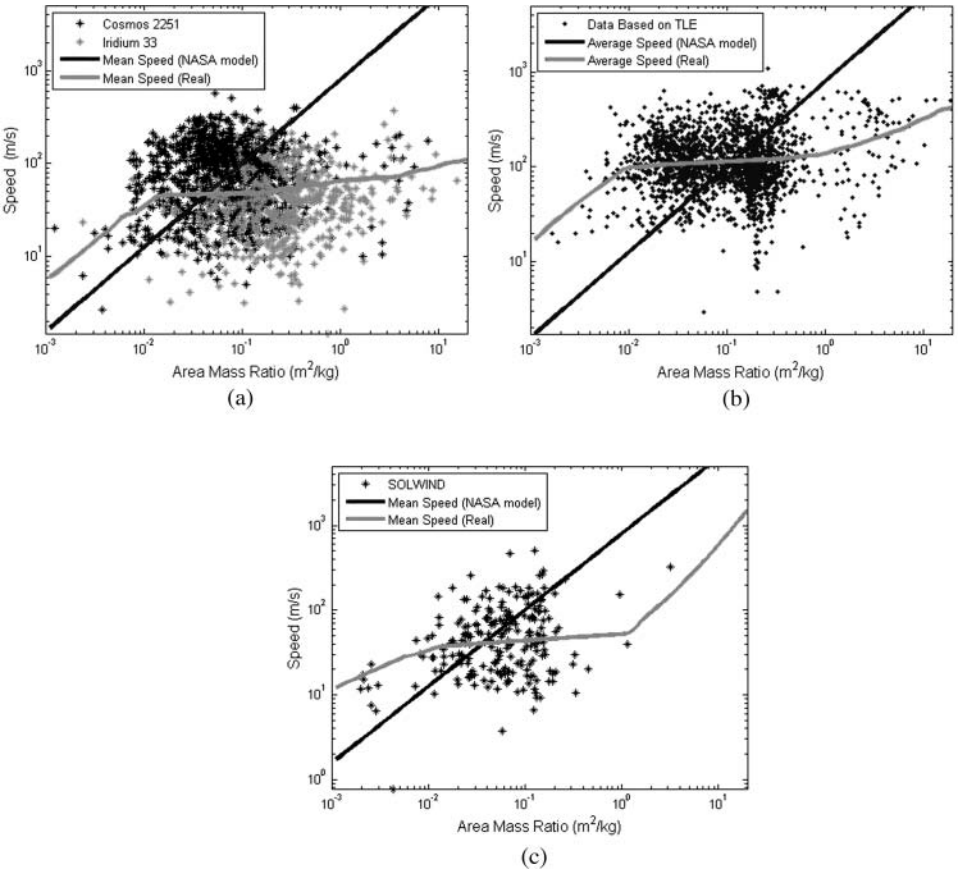


**Figure 7:** Distribution with A/M and relative speed. The dots show the actual values for the fragments from the Iridium-Cosmos collision on the top left, from the Fengyun breakup on the top right, and from SOLWIND on the bottom left. The dark line shows the relationship between relative speed and A/M predicted by the NASA model. The light curve is the mean speed determined by locally weighted. (a) Cosmos 2251—Iridium 33; (b) Fengyun (c) SOLWIN.

that the relationship between A/M and relative speed in the NASA model is not generally correct.

Figure 8 shows the velocity distribution of catalogued fragments along three directions. The velocity components are defined relative to the satellite body coordination system shown in Figure 9.[13] The azimuth in the figure is the angle between the x-axis and the projection of the velocity vector on the x-y plane; the elevation is the angle between the velocity vector and the x-y plane.

The curves in Figure 8 indicate that the directions of the relative velocities of the Iridium fragments are essentially randomly distributed since the distributions are centered around zero. However, the distribution of velocities of Cosmos fragments is shifted in the positive z direction and negative x direction.

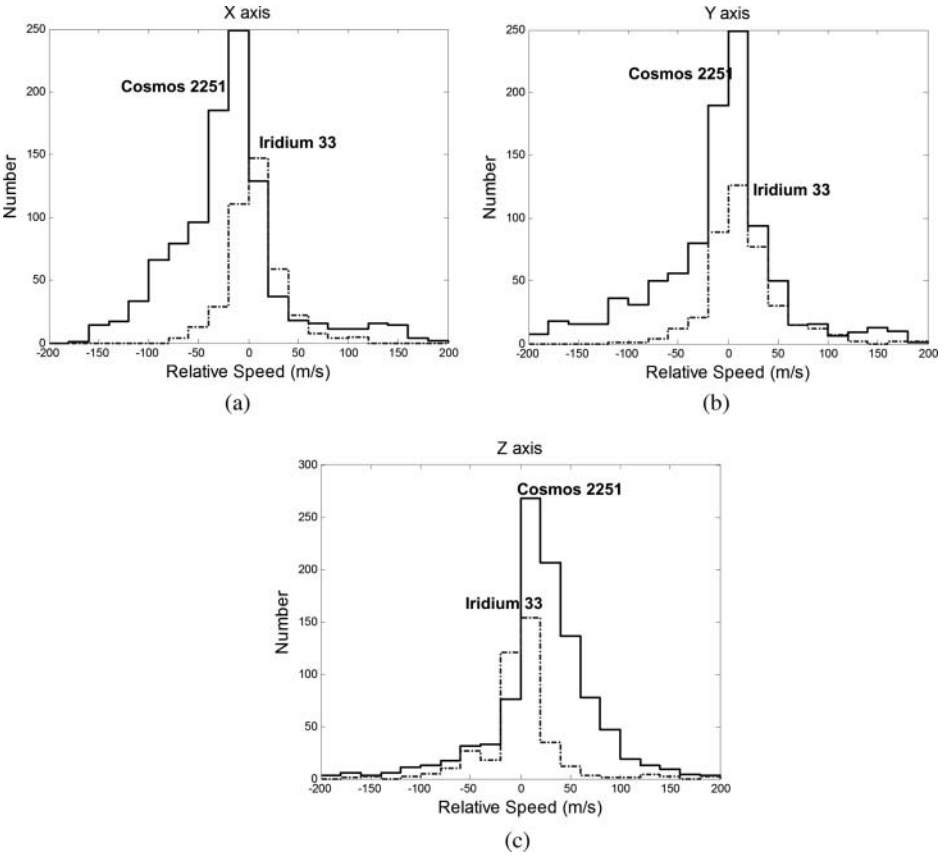


**Figure 8:** Distribution of the components of relative velocity along three axes. The axes are shown in Figure 9.

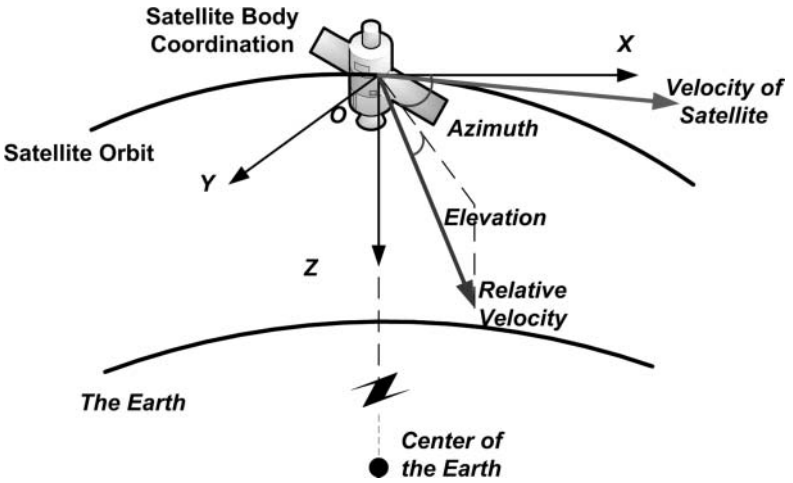


**Figure 9:** Satellite body coordination, and azimuth and elevation angles.

These shifted velocity distributions cannot result from momentum transfer from Iridium since the Iridium distributions do not show a corresponding shift.

As noted above, untrackable fragments may account for more than 20% of the Cosmos mass. Moreover, smaller fragments may on average have larger values of A/M than large fragments,[14] and according to the observation results (see Figure 7) would be expected to gain higher relative speeds than larger fragments. Therefore, these missing fragments could carry enough momentum to account for the apparently missing momentum.

If this is true, the direction distribution of relative velocity of the untrackable fragments must be quite different from that of the catalogued fragments. Using conservation of momentum to determine the relative velocity distribution of the untackable fragments could be useful for refining models of debris produced by breakups.

## LIFETIME AND ORBITAL EVOLUTION OF THE IRIDIUM-COSMOS FRAGMENTS

Calculating the lifetime and orbital evolution of the cataloged fragments from the Iridium-Cosmos collision is useful for understanding the long-term hazard they pose to other objects.

A semi-analytical lifetime algorithm is developed to calculate orbital lifetime of the catalogued fragments produced in this event.[15] Inputs to this algorithm include A/M of the fragments as calculated in section 2.2, the published TLE data for the fragments, and a detailed atmosphere model (NRLMSIS 00). Solar flux data (F107) and geomagnetic index data (KP) for the last 4 solar cycles (1965–2009) are averaged, and served as input for the atmosphere model.

The algorithm calculates the variation of the semi-major axis and eccentricity of the orbit of each fragment, taking into account atmospheric drag and so-called J2 perturbations due to the non-sphericity of the Earth. The calculation then determines which fragments decay with time. Checking this algorithm with the known fragment lifetimes from the 1985 Ariane breakup shows that the error in the estimated lifetime (including errors from the A/M calculation) for a specific fragment is about 15%.

The results are shown in Figure 10. Because there is very little atmospheric drag at the high altitude where this collision occurred, a large fraction of the debris created will stay in orbit for several decades. Roughly one-fifth of the catalogued fragments from this collision will remain in orbit more than 30 years. Fragments from the Cosmos satellite have longer lifetimes due to lower area-to-mass ratio. The irregularity of the curves is due to effects of the 11-year solar cycle.

Because the collision occurred several hundred kilometers above the International Space Station (ISS), this debris is unlikely to pose a large, near-term

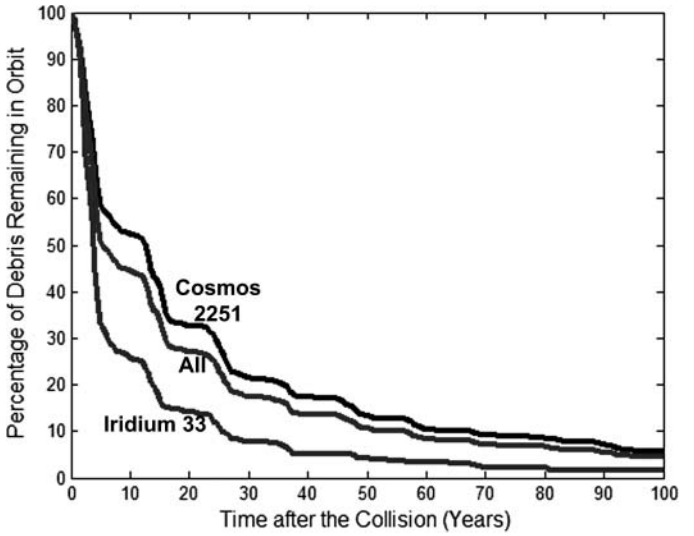


**Figure 10:** Fraction of debris that is expected to remain in orbit as a function of time after the collision.

risk to the ISS. On the other hand, over the next 10 to 20 years—which is the predicted ISS lifetime—about 70% of the catalogued fragments will decay and pass through the ISS orbit. This represents a small but long-term risk to the ISS.

Because of the relative speeds given to the fragments by the collision, the fragments will have a distribution of orbital speeds, most of which differ from the orbital speed of the original satellite by a few percent (see Figure 6). As a result, after the collision the debris from each satellite first spreads out along the orbit of the original satellite. The non-sphericity of the Earth causes the orbits to precess slowly and in time the debris spreads to form a shell around the Earth (Figure 11). The fragments remain concentrated near the altitude at which the original satellites orbited. Since the Cosmos fragments have larger relative speeds and lower orbital inclinations than the Iridium fragments, they will precess faster. As a result, the orbits of the Cosmos fragments will spread out more quickly and will be distributed around the Earth within 3 years. However, even though they are spreading more slowly, the Iridium fragments still pose a threat to all satellites that pass through that altitude.

## EFFECT OF THE IRIDIUM-COSMOS COLLISION ON THE SPACE ENVIRONMENT

In this section, the short- and long-term effects of this collision on the space environment are estimated. Here "short-term effects" means the collision risk

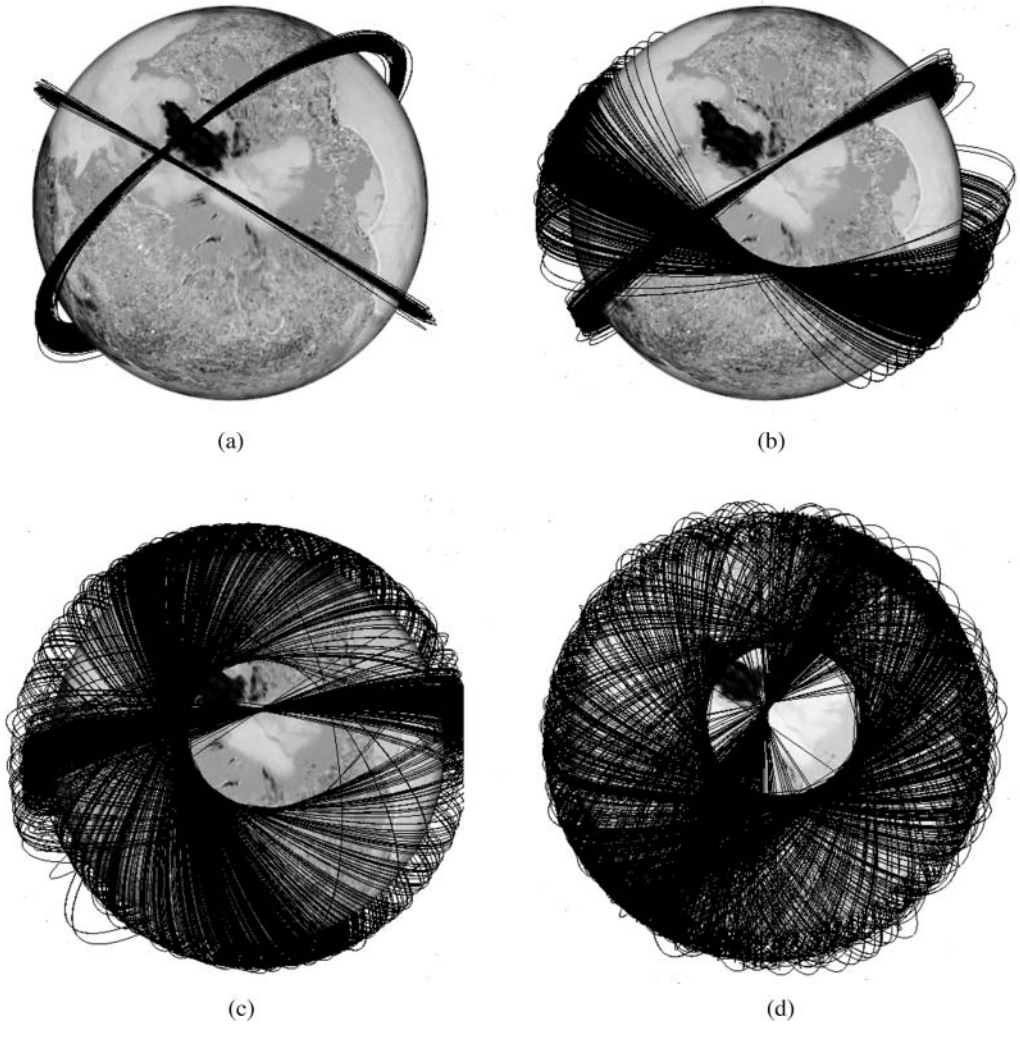


**Figure 11:** Spread over time of debris orbits from the collision. Most fragments created by the collision have orbital speeds that are close to the speed of their parent satellite, and therefore follow orbits that are close to the orbit of the parent satellite. The distribution of fragment speeds cause the fragment orbits to process at different rates; more of the Cosmos fragments have higher relative speeds and lower inclination than the Iridium fragments, so the Cosmos orbits spread faster. By three years after the collision, the Cosmos fragments are spread into a shell around the Earth, concentrated at the altitude of the original Cosmos satellite. (a) 7 days after the collision; (b) 3 months after the collision; (c) 1 year after the collision; (d) 3 years after the collision.

for objects in space posed by the cataloged Iridium-Cosmos fragments within 1 year after the collision.

## Short Term Effect on Space Environment

The collision risk of a spacecraft with other space objects is proportional to the number of conjunctions between them, where a conjunction refers to an event in which the two objects pass within some specified "critical distance" of each other.

To analyze the collision risk resulting from collision fragments, the number of conjunctions is calculated in a 24-hour period between all intact orbiting objects (spacecraft and upper-stages of launch vehicles) with all objects that are contained in the SSN catalog as of 17 November 2009.[16] For this calculation, a conjunction is defined as two object passing within 5 km of each other.

Since there are some 15,000 objects in the catalog, the conjunction algorithm applies several filters to reduce the amount of computation required, based on the relative geometry of pairs of objects. For example, the algorithm filters out pairs of objects on orbits with altitudes that are separated by at least the critical distance. By applying these filters, calculating conjunctions between tens of millions of pairs of objects over a 24-hour period requires only 10 minutes for an ordinary PC.[17]

The result is shown in Figure 12. There are 3,222 conjunctions of intact objects with all catalogued objects during the 24-hour period on 17 November 2009. Of these, 2530 took place with objects other than fragments from

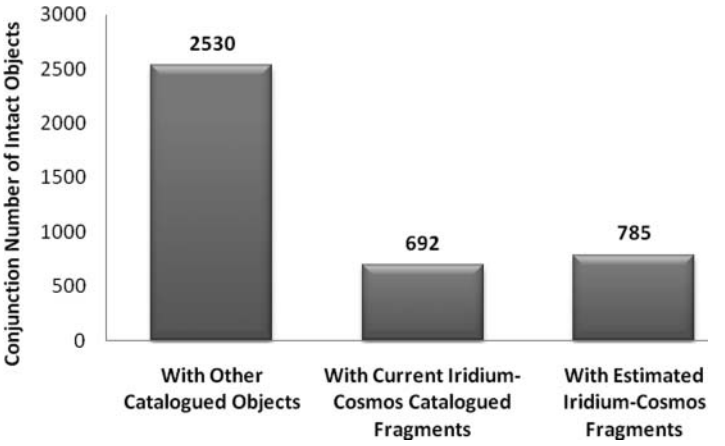


**Figure 12:** Number of one-day conjunctions of intact objects with other objects. The left bar shows the number of conjunctions of intact objects with cataloged objects other than fragments from the Iridium-Cosmos collision. The middle and right bars show the number of conjunctions of intact objects with the currently cataloged fragments from the Iridium-Cosmos collision and with the estimated total number of fragments larger than 10 cm from that collision. The calculations use the data from the SSN catalog on 17 November 2009.

the Iridium-Cosmos collision, so this is the number of conjunctions one would expect if the Iridium-Cosmos collision had not occurred.

The remaining 692 are conjunctions of intact objects with catalogued fragments from the Iridium-Cosmos collision. It is estimated above that roughly 13% of fragments from the Iridium-Cosmos collision have not been cataloged (see Table 1); including these additional fragments increases the number of conjunctions from 692 to 785.

These results mean that the Iridium-Cosmos collision resulted in a 25 to 30% increase in the risk to intact objects of collisions with catalogued objects.

Figure 13 shows the distribution with altitude of these conjunctions. This shows that the collision risk of intact objects with all cataloged objects in the altitude band of 700 to 800 km—which was already the most dangerous region of space—doubled after the Iridium-Cosmos collision. The number of conjunctions at ISS orbit (below about 450 km altitude) is low since the lifetime of objects is short at those attitudes due to high atmospheric drag.

## Long-Term Effects on the Space Environment

The negative long-term effect of the Iridium-Cosmos fragments on the space environment is a major concern of the space-faring nations. In this section, the long-term cumulative number of collisions between intact objects and fragments larger than 10 cm from the Iridium-Cosmos collision are estimated.

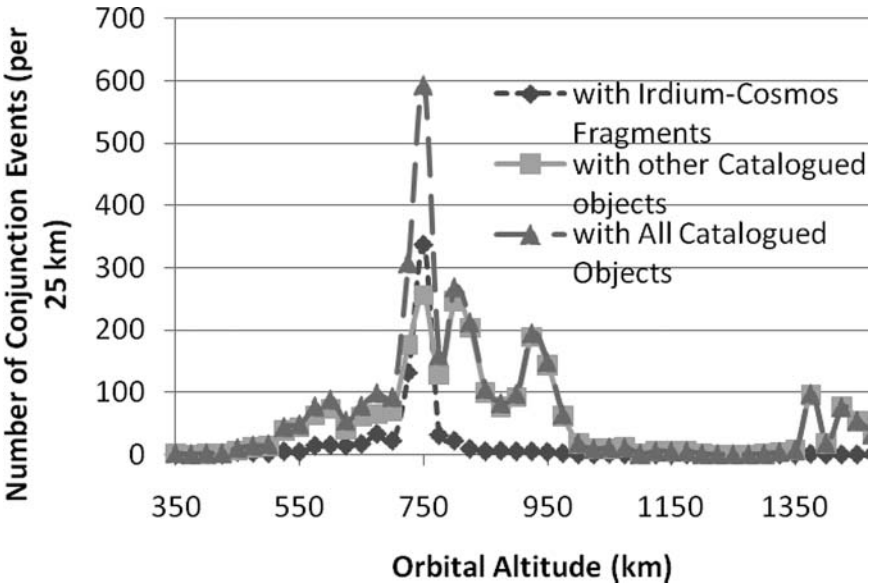


**Figure 13:** Distribution with altitude of conjunctions between intact objects and cataloged debris (on November 17, 2009).

**Table 3:** Historical collisions between cataloged objects[1]

| | |
|---|---|
| Dec 1991 | Inactive Cosmos 1934 satellite (Catalog Number 18985) hit by debris from Cosmos 296 satellite (Catalog Number 13475) |
| July 1996 | Active French Cerise satellite (Catalog Number 23606) hit by debris from Ariane rocket stage (Catalog Number 18208) |
| Jan 2005 | U.S. rocket body (Catalog Number 7219) hit by cataloged debris from Chinese rocket stage (Catalog Number 26207) |
| Feb 2009 | Active Iridium 33 satellite (Catalog Number 24946) hit by inactive Cosmos 2251 satellite (Catalog Number 22675) |

[1]N. L. Johnson et al., "History of On-orbit Satellite Fragmentations 14th Edition," Lyndon B. Johnson Space Center, Houston 2008.

To assess the risk of collisions, two estimates are used for the collision rate of cataloged intact objects with all cataloged space objects. One estimate comes from the number of observed collision events. The other estimate comes from a NASA analysis that used NASA's LEGEND model.[18] The collision rate in this analysis is calculated for 1 January 2006, which is the time NASA's calculation starts.

For the first estimate, there have been three intact-fragment collisions and one intact-intact collision in the last 20 years (Table 3), and that was used to calculate the average collision rate over the last 20 years.[19] The top row of Table 4 shows the mean number of collisions per year assuming this collision rate.

For the second estimate, a 2006 NASA analysis is used, which estimated potential collisions between objects larger than 10 cm over the next 200 years.[9] NASA estimated that over the next 200 years, the mean number of collisions between two intact objects will be 4.9, and between intact objects and fragments will be 10.8. Essentially all these collisions are in LEO. NASA's calculation was done assuming 7,667 objects in orbit, roughly 2,500 of which were intact objects. Since the number of catalogued objects in LEO in 2006 was in fact about 6,100, their results are scaled to this number of objects.[20] Assuming the additional 1,600 objects are fragments, the intact-intact collision number will remain the same, but the intact-fragment collision number will decrease to $10.8 * (6{,}100–2{,}500)/(7{,}667–2{,}500) = 7.5$ in next 200 years. According to NASA's

**Table 4:** Estimates of one-year mean numbers for collisions between cataloged objects on Jan 1st 2006. The first column is for collisions between two intact objects and the second column is for collisions between an intact object and a fragment

| | Intact-Intact | Intact-Fragment | Sum |
|---|---|---|---|
| Number from Actual Events | 0.050 | 0.15 | 0.20 |
| Number Estimated by NASA | 0.025 | 0.038 | 0.062 |

analysis, the collision rate increases slightly with time but is relatively stable over the next 200 years. The mean collision number on 1 January 2006 is assumed to be equal to the mean collision number over 200 years. The results as shown in the bottom row of Table 4.

The overall NASA collision rate (the Sum column in Table 4) is three times smaller than that estimated from the observed collisions. One might assume this is related to the large increase in collision fragments since 2006, but none of the observed collisions involve these additional fragments. Moreover, the fragment population during the 1990s was 10% smaller than that in 2006, and that factors into the 20-year average used to calculate the top row in Table 4. To demonstrate that the collision rates estimated from the NASA report represent a lower bound on the actual historical collision rates, the following calculation shows that these rates do not account well for the observed number of collisions.

According to probability theory, if $\lambda$ is the mean number of collisions in a given time span, then the probability of exactly $k$ collisions occurring during that time span is given by the Poisson distribution:

$$p_\lambda(k) = \frac{e^{-\lambda}\lambda^k}{k!} \tag{2}$$

These probabilities are calculated for different values of $k$ assuming the NASA collision rates. If NASA's estimate of the mean collision rate is correct, then the mean number of collisions between intact objects and all objects is 1.57[21] over the span of 20 years, instead of the four actually seen. Figure 14 shows the probability of seeing different numbers of collisions over 20 years assuming the NASA collision rate, calculated using Eq. (2). In this case, the probability of having four collisions in 20 years is about 3%, which suggests that the NASA analysis may underestimate the collision probability.

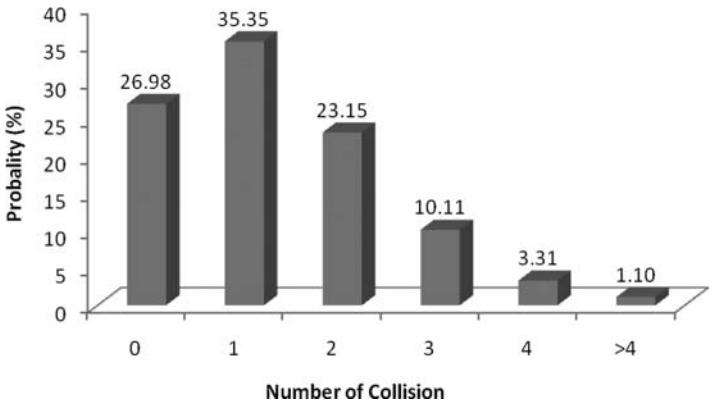


**Figure 14:** The probability of seeing different numbers of collisions in 20 years, assuming NASA's value of the collision probability (0.0785) from Table 4.

This underestimate may result in part from uncertainties in the size and shape of objects in space, and the fact that the NASA model may not take into account how collision probability varies with the shape of the two objects. The shape effect is considered in Appendix B. That analysis shows, for example, that for objects with the same surface area, the collision probability between two spheres is significantly smaller than between two long rods. Approximating all objects as spheres in the collision model would therefore underestimate the actual collision probabilities.

In particular, it is important to note that the NASA's LEGEND model does not consider collisions with satellite appendages (e.g., booms or solar panels).[22] However, collisions between satellite appendages and intact objects could result in catastrophic collisions that produce large amounts of debris. Indeed, the Iridium-Cosmos collision may have involved an appendage of the Iridium satellite. If the collisions involving appendages (the Cerise collision and maybe the Iridium-Cosmos collision) are excluded, the collision rate agrees with NASA's estimation, since the probability for 2 collisions in last 20 years is more than 20% (see Figure 14).

On the other hand, using the collision rate in the top row of Table 4 (0.20) there is a 20% probability of seeing four collisions. For the analysis below, the two sets of collision rates are used in Table 4 as low and high values for comparison.

As a first step in estimating the number of future collisions, the number of conjunctions between intact objects and other cataloged intact objects and fragments on 1 January 2006 is calculated. The results are shown in Figure 15. For comparison, the number of conjunctions on November 17, 2009 is also calculated, which was given above in Figure 12. The dramatic increase in conjunctions is due to the rapid increase in the number of objects in the SSN catalog, which increased from about 9,400 to 15,000 over that time. The growth of

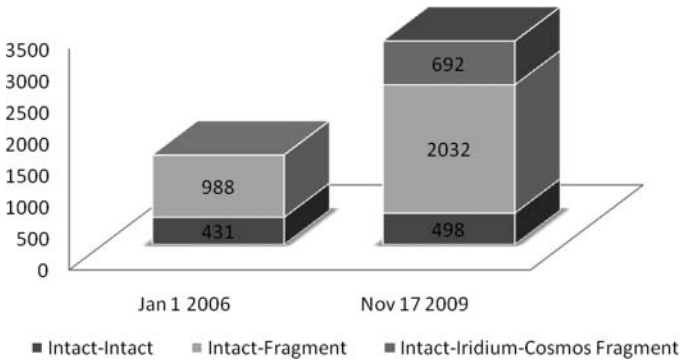


**Figure 15:** Number of conjunctions of different types in 24-hour periods on 1 January 2006 and 17 November 2009.

the catalog included an increase in the number of intact objects by about 500 and of fragments by about 5,000.

The cumulative mean collision number between intact objects and fragments from the Iridium-Cosmos collision can be estimated by

$$C = \int \gamma \frac{N_c}{N_{2006}} K dt \tag{3}$$

where:

$N_c$ is the one-day number of conjunctions between intact objects and the catalogued fragments from the Iridium-Cosmos collision, which can be determined from Figure 12.

$\gamma$ is the fraction of Iridium-Cosmos fragments remaining in orbit, from Figure 10.

$N_{2006}$ is the one-day number of conjunctions between intact objects and cataloged fragments on January 1, 2006, which can be found from Figure 15.

$K$ is the mean number of collisions per year of intact objects with fragments, which is given in Table 4.

Equation (3) assumes that the number and the orbits of intact objects do not change over the integration time. This a conservative assumption since the number of intact object increases due to new space launches, and that will increase the number of collisions. In addition, Eq. (3) does not include secondary collision fragments produced by collisions with the original Iridium-Cosmos fragments.

Equation (3) is used to calculate the cumulative mean number of collisions between intact objects and cataloged Iridium-Cosmos fragments for the two values for the collision probabilities given in Table 4. The results are shown in the Figure 16.

Figure 16 shows that in the next 100 years, the mean number of collisions of intact objects with the large Iridium-Cosmos fragments would be 0.5 to 2. In addition, if an on-orbit collision happens, it will probably happen within 30 years after the Iridium-Cosmos collision, since 80% of the fragments are expected to decay during that time. As noted above, since the number of intact objects is expected to increase over this time period, this estimate is a lower bound, but gives an indication of the impact of these fragments on the space environment.

Moreover, the number of Iridium-Cosmos fragments with size between 1 and 10 cm is expected to be roughly 50 times greater than the number of fragments larger than 10 cm. As a result, many tens of collisions are expected between intact objects and Iridium-Cosmos fragments greater than 1 cm.

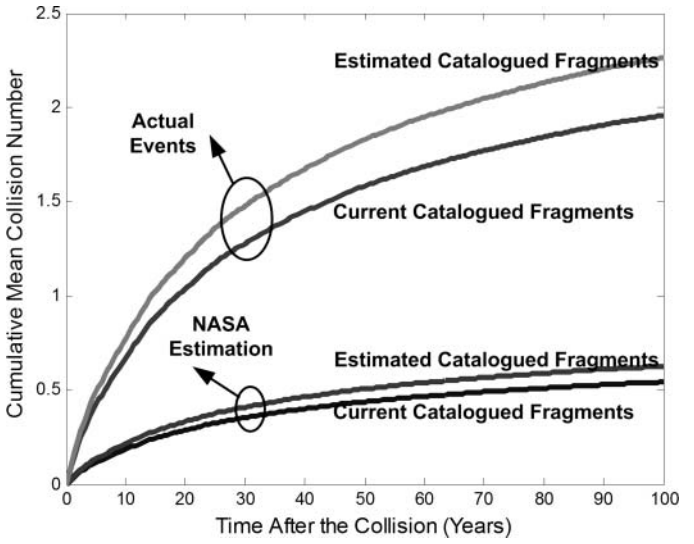


**Figure 16:** Cumulative mean number of collisions between intact objects and Iridium-Cosmos fragments larger than 10 cm. The lower two curves assume the lower value of the collision probability given in Table 4 (0.062), and the upper curves assume the higher value (0.20). For each pair of curves, the lower curve assumes the number of Iridium-Cosmos fragments currently cataloged and the upper (gray) curve assumes the possible total number of fragments larger than 10 cm.

If the mass and collision speed are high enough, collisions with fragments larger than 10 cm may carry enough kinetic energy to completely fragment an intact object. This would create a cloud of fragments that would also create a similar collision risk. In principle, with good enough tracking data, close conjunctions between cataloged objects can be predicted and in some cases steps can be taken to reduce the chance of collision.

While fragments around 1 cm in size are unlikely to have enough mass to cause an intact object to break up, they can seriously damage or disable an active satellite. Since fragments of this size are too small to be tracked reliably, possible collisions cannot be predicted. Moreover, fragments larger than 1 cm colliding with an object at orbital speeds cannot be effectively shielded against. So because they are numerous, destructive, and cannot be tracked, fragments of this size pose a particular threat.

## CONCLUSIONS

The analysis of the Iridium-Cosmos collision, using observational data on the debris fragments from the U.S. Space Surveillance Network, concludes that the collision created roughly 1,850 fragments with size greater than 10 cm. The number of fragment with size greater than 1 cm is probably greater than 100,000.

Roughly one-fifth of the cataloged fragments are expected to remain in orbit more than 30 years, and roughly 5% of fragments have orbital lifetimes longer than 100 years. The fragments from the Iridium satellite will on average have a significantly shorter lifetime than Cosmos fragments, possibly due to fact that fragments from the Iridium solar panels may have a relatively high area-to-mass ratio.

The bulk of the Iridium satellite appears to be intact, implying that Iridium may have been struck a glancing blow rather than a direct collision to the body of the satellite.

Because of the large number of fragments created, the Iridium-Cosmos event increased by 25% the risk that intact objects in orbit would be hit by an object larger than 10 cm in the year following the collision. The largest increase in collision risk is at altitudes of 700 to 800 km, which was already the most dangerous region. However, this debris will not significantly increase the risk to the International Space Station, which is at a much lower altitude.

The number of collisions between cataloged objects that have occurred in the past 20 years suggests a higher collision probability—for a given number of cataloged objects in orbit, and therefore for a given number of conjunctions—than has been assumed in some past studies. This would imply that collisions in space will happen more frequently than previously expected.

A higher collision probability may result from underestimates of the size of objects in orbit, as well as a failure to take into account the shape of these objects, which is shown to significantly influence the collision probability. An accurate estimate of the collision probability is important for understanding the long-term evolution of space debris.

In addition, the large increase in space debris from breakup events has doubled the number of daily conjunctions since 2006. Both the increase in the number of conjunctions and a higher collision probability for a given number of conjunctions will lead to more collisions in coming years than predicted in past studies.

The mean collision number is estimated to be 0.5 to 2 in next 100 years between intact objects and those Iridium-Cosmos fragments larger than 10 cm (under the conservative assumption that the number of intact objects remains constant). Since the number of fragments with size between 1 and 10 cm is 50 times larger than the number larger than 10 cm, it is estimated that there will be many tens of collisions between intact objects and Iridium-Cosmos fragments greater than 1 cm.

Our analysis also has implications for NASA's Standard Breakup Model. The cumulative fragment number as a function of fragment size is found to follow a power law relationship, as the NASA model indicates, but the parameters of the power law depend on the breakup event. The NASA model can therefore over- or under-predict the debris from a particular event in different size ranges.

The calculations in section 2.4 indicate that the NASA Standard Breakup Model probably is not correct in estimating the velocity of fragments from the collision relative to A/M. In this case, the model does not appear to give the correct functional form.

Both of these issues are important for using the NASA model for long-term simulations. Incorporating data from the breakup events in recent years should lead to improvements in the NASA model.

The Iridium-Cosmos event highlights the fact that collisions in space are not just theoretical, but are a real risk for space assets. The international community has taken steps in the right direction by developing debris mitigation guidelines for routine activity in space. These guidelines have been adopted by the United Nations, and should be obeyed by all space-faring countries.

However, even if these measures are followed, the debris population will likely continue to increase in some regions of space. The calculations in section 4.2 suggest that the collision risk in space may be higher and the debris population may increase more quickly than previously expected. Preventing that will require reducing the amount of debris in orbit, which may require removing existing large, massive objects from orbit.

## ACKNOWLEDGEMENTS

The author wishes to thank David Wright and Prof Hai Huang for discussions and comments on this paper.

The author acknowledges support from the John D. and Catherine T. MacArthur Foundation through a grant to the Peace Studies Program, Cornell University. Early stages of this research were supported in part by a grant from the John D. and Catherine T. MacArthur Foundation to the Space Working Group at Beihang University in Beijing.

## REFERENCES

1. N. L. Johson et al., "NASA's New Breakup Model of Evolve 4.0," *Advances in Space Research* 28 (2001): 1377–1384.

2. G. Stansbery et al., "A Comparison of Catastrophic On-Orbit Collisions," Proceedings of the Advanced Maui Optical and Space Surveillance Technologies Conference, Wailea, Maui, Hawaii, 2008.

3. J.-C. Liou and N.L. Johnson, "Characterization of the Cataloged Fengyun-1C Fragments and Their Long-term Effect on the LEO Environment," *Advances in Space Research*, 43 (2009).

4. For more information about TLEs, see http://en.wikipedia.org/wiki/Two-line_element_set

5. These past events are the breakup of the Fengyun 1C (International ID 1999–025) in 2007, breakup of the rocket body Ariane (International ID 1994-29B) in 1996, and breakup of the P-78 (Solwind) (International ID 1979-017A) in 1985.

6. E. G. Stansbery, "Growth in the Number of SSN Tracked Orbital Objects," (paper presented at the 55th International Astronautical Congress, Vancouver, Canada, 2004).

7. The ratio is calculated from the space situation report of www.space-track.org, on 7 July 2009 (accessed 7 May 2010).

8. H. Klinkrad, *Space Debris Models and Risk Analysis* (Verlag: Springer, 2006).

9. Y.-I. Xu et al., "A Statistical Size Estimation Model for HAYSTACK and HAX Radar Detections," (paper presented at the 54th International Astronautical Congress, 2005).

10. T. Wang and H. Huang, "Estimating Orbital Lifetime of Space Objects from Two-line Elements," (paper presented at the 3rd IAASS Conference, Rome, 2008).

11. Details of the atmosphere model can be found at http://www.nrl.navy.mil/research/nrl-review/2003/atmospheric-science/picone/ (accessed 7 May 2010).

12. L. Anselmo and C. Pardini, "Analysis of the Consequences in Low Earth Orbit of the Collision between Cosmos 2251 and Iridium 33," Paper presented at the 21st International Space Flight Symposium, Toulouse, France, 28 September–2 October 2009.

13. The z-axis of the coordination system always points from the fragment along Earth radius vector toward Earth's center. The x-axis of the coordination system points in the direction of the velocity vector and is perpendicular to the radius vector (if orbital eccentricity is zero then the direction of the x-axis and that of the velocity vector are the same). The y-axis is normal to the orbital plane.

14. For example, for a sphere of radius r, A/M $\sim$ 1/r, which increases as r decreases.

15. T. Wang and H. Huang, "New Method to Determine Close Approaches Between Satellite," (paper presented at the 3rd IAASS Conference, Rome, 2008). Available at http://wangting.org/pages/papers/close%20approach.pdf (accessed 21 June 2010).

16. For the analysis described below in the paper, the data in the SSN catalog, and used by following calculations are on the same day, which was 17 November 2009.

17. T. Wang and H. Huang, "New Method to Determine Close Approaches Between Satellite," (paper presented at the 3rd IAASS Conference, Rome, 2008).

18. J. C. Liou and N. L. Johnson, "Instability of the Present LEO Satellite Populations," *Advances in Space Research* 41 (2008): 1046–1053.

19. Since there are only four observed collisions with intact objects since space activities began, people may argue a longer time span should be used here, rather than 20 years. However, the collision rate several decades ago was low, due to a smaller population of objects in orbit. For example, there were only about 700 intact objects in orbit in 1970 and 1,700 in 1980, compared to 3,000 in 1990 and 4,500 today. In addition, even if a collision involving an intact object occurred, it might not have been detected since the computational capacity was low and the collision algorithms were inefficient before 1990. Consider that seven collisions have been discovered after 1997, and none before that (the Cosmos 1934 collision in 1991 was not discovered until 2005, and three other possible collisions were detected in 1997, 2002 and 2008; these are believed to be collisions with untrackable objects.). Moreover, even if the four collisions are considered to have occurred in 25–30 years, that would still give a collision probability that was twice the value NASA uses.

20. On 1 January 2006, there were 532 catalogued objects whose orbits are not published. These were U.S. military satellites and mission-related fragments and rocket bodies from the launch of these satellites. Many of these objects are in LEO, but due to the lack of orbit information, these objects are not included in following calculations.

21. There are several thousand fragments tracked by SSN that are not in the catalog, since their source is unknown. These fragments are used in the NASA LEGEND model.

Since no collisions have been observed between intact object and these tracked but uncataloged objects, it is appropriate to use the collision rate of all objects considered by NASA, 1.57 (= (4.9 + 10.8)/200 * 20), instead of using collision rate of catalogued objects, 1.2 (= (4.9 + 7.5)/200 * 20).

22. J.C. Liu, "An Updated Assessment of the Orbital Debris Environment in LEO," *Orbital Debris Quarterly News* 14 (2010). This article argues that satellite appendages can be neglected because collisions between satellite appendages and debris may cause problems for operational payloads, but would have negligible contribution to the growth of the debris population. However, as noted in the text, collisions between satellite appendages and intact objects could produce large amounts of debris.

## APPENDIX A. METHOD TO DETERMINE THE RELATIVE VELOCITY OF FRAGMENTS

Method to calculate relative velocities of the fragments are discussed, which is created by a collision between two objects. The satellite is assumed to have been tracked by the SSN, so its orbit is accurately known. Since the time of the collision is known, the position $\mathbf{r}_s$ and velocity $\mathbf{V}_s$ of the spacecraft at the time of the collision can be determined to high accuracy.

However, tracking of fragments may not begin until some time after the collision, so their orbits just after the collision are not known well enough to determine their positions and speeds accurately at that time. The method to determine the initial relative velocities of the fragments is described here.

First, the TLEs are used to determine the trajectory of each cataloged fragment. Then, at the time of the collision, the fragment is assumed to be at the point on its estimated orbit that is closest to the location of the spacecraft at that time (see Figure A-1).

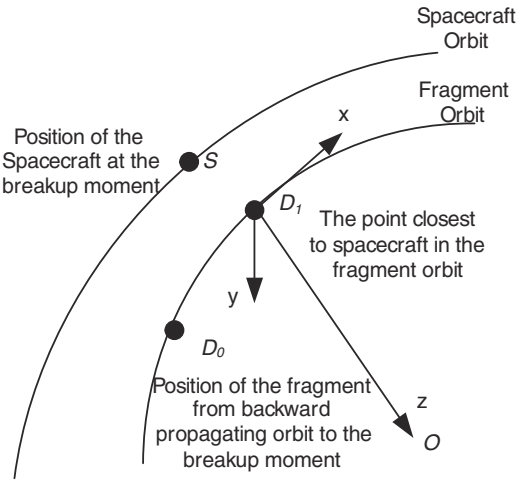


**Figure A-1:** The relationship between spacecraft orbital and fragment orbit at the breakup moment.

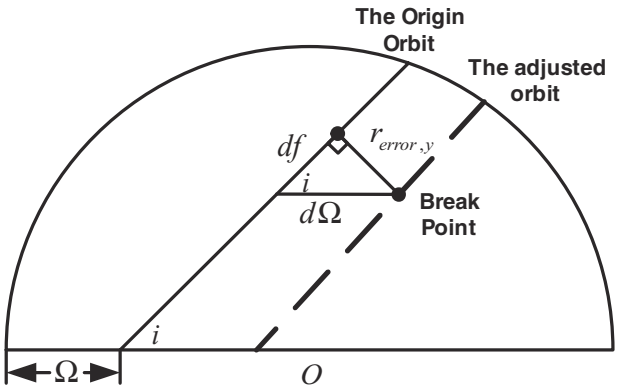


**Figure A-2:** Sketch of adjusting orbits.

The position of the closest point is $\mathbf{r}_{deb}$ and the corresponding velocity is $\mathbf{V}_{deb}$. Due to uncertainties in the orbits, $\mathbf{r}_{deb}$ and $\mathbf{r}_s$ will typically not be the same. the values of $\mathbf{r}_{deb}$ and $\mathbf{V}_{deb}$ using the following method.

A satellite coordinate system[1] can be established from $\mathbf{r}_s$ and $\mathbf{V}_s$. In the satellite coordinate system, the error $\mathbf{r}_{error}$ in the fragment's position and its relative velocity $\mathbf{V}_{rel}$ can be expressed by:

$$\begin{aligned} \mathbf{r}_{error} &= \mathbf{C}_{oi}(\mathbf{r}_{deb} - \mathbf{r}_s) \\ \mathbf{V}_{rel} &= \mathbf{C}_{oi}(\mathbf{V}_{deb} - \mathbf{V}_s) \end{aligned} \tag{1}$$

where $\mathbf{C}_{oi}$ is a matrix that transforms the inertial coordinate system to the satellite coordinate system.

In an ideal situation, $\mathbf{r}_{error}$ would be zero. However, $\mathbf{r}_{error}$ is typically nonzero due to orbital propagating errors. Choosing the fragment position at the breakup time eliminates as the point on the orbit closest to $\mathbf{r}_s$ eliminates most of the error along the trajectory, i.e. $\mathbf{r}_{error,x}$. Therefore, it is only needed to minimize the other components, $r_{error,y}$ and $r_{error,z}$.

As noted above, since the spacecraft's orbit is known accurately and requires a short orbital propagation back to the time of the collision, presume that $\mathbf{r}_s$ is known accurately and that $\mathbf{r}_{deb}$ is the only source of error in $\mathbf{r}_{error}$.

The component $r_{error,z}$ is determined by errors in the semi-major axis and eccentricity of the fragment's orbit. Atmospheric drag and solar pressure are the main sources for these errors. In the standard SGP4 model used to determine orbits from TLEs, $B^*$ is the TLE parameter that reflects the impacts of atmosphere drag and solar pressure. $B^*$ is calculated by fitting the satellite orbit to observational data collected over several days, and therefore only reflects these perturbations over a relatively short time. However, in some cases, the orbit must be propagated backwards by tens of days, and using $B^*$ would lead

to a large error. Changing $B^*$ will change the semi-major axis, eccentricity and hence $r_{error,z}$. Therefore, a Newton-iteration method is used to minimize $r_{error,z}$ by varying $B^*$, using the value of $B^*$ from the TLEs as the initial value.

To eliminate $r_{error,y}$, $\mathbf{r}_{deb}$ and $\mathbf{V}_{deb}$ is firstly be transferred into classical orbital elements. From the geometry, $r_{error,y}$ is determined by the right ascension of the ascending node $\Omega$ and orbital inclination $i$. In considering the effects of J2 perturbations, $\Omega$ is a "fast" variable, usually changing several degrees a day, while changing $i$ by several degrees could take several years. Calculations show that the error of $\Omega$ could be ten times greater than that of $i$. Therefore, it is reasonable to assume that $r_{error,y}$ is only determined by $\Omega$. As a result, $r_{error,y}$ is eliminated by changing $\Omega$. Figure A-2 illustrates the orbit adjustment. As shown in the figure, changing $\Omega$ will lead to variation of true anomaly $f$. From the geometry, $d\Omega$ and $df$ can be expressed by:

$$\begin{aligned} d\Omega &= \pm \frac{\sin(r_{error,y}/r)}{\sin i} \\ df &= \pm \arccos\left[\frac{\cos d\Omega}{\cos(r_{error,y}/r)}\right] \end{aligned} \tag{2}$$

Where, $r$ is the center distance, from the Earth center to the fragment.

The adjusted values of $\Omega$ and $f$ can be obtained from iterating Equation (2) several time

In the proposed algorithm, $B^*$ is firstly be adjusted to decrease $r_{error,z}$, The second step is to use Equation (2) to eliminate $r_{error,y}$ and determine the orbital elements at the time of breakup. The final step is to transform back from orbital element to the velocity $\mathbf{V}_{deb}$, and then use Equation (1) to calculate the relative velocity $\mathbf{V}_{rel}$.

## APPENDIX B. LONG TERM COLLISION PROBABILITY BETWEEN OBJECTS WITH DIFFERENT CROSS-SECTION SHAPES

For collisions between a large object and a small particle, the probability of collision is almost unrelated to their shape. However, for objects with similar sizes, the shape can strongly influence the collision probability.

Russell proposed a method to calculate short-term collision probabilities between objects and a specific spacecraft having a complicated shape.[2] His method is widely used in collision avoidance. However, his method assumes that the attitude of the spacecraft is fixed, and therefore cannot be used to estimate the long-term average collision probability, which assumes the attitude of the spacecraft is random. Kessler calculated the long-term collision probability of an object assuming the object is equivalent to a sphere having the same surface area as the object, based on the assumption that randomly distributed attitude would eliminate the influence of shape.[3]

In this section, a Monte Carlo simulation is used to understand how long term collision probability depends on the shape of the colliding objects. The results indicate that Kessler's assumption is not correct.

## B.1 Method

A Monte Carlo method is used to study the collision probabilities between spheres and cylinders with the same surface area. The calculation can be divided in three sections:

1. A two-dimensional array is created, and its elements are initially set to zero. The array represents a two-dimensional field.
2. Choose two objects (each either a sphere or a cylinder of specified shape, but all having the same surface area) and place them in random positions, with random elevation $\alpha$ and random azimuth $\beta$ with respect to the two dimensional field (please see Figure B-1). The objects are much smaller then the two-dimensional field.
3. Project the objects onto the two-dimensional field and add the number one to the value of all array elements that are part of the projected areas (Figures B-1 and B-2). (The projection of a cylinder is a combination of a rectangle and two ellipses, and the projection of a sphere is a circle.) On the two-dimensional array, the elements with zeros are the places where there is no object, the elements with ones are the areas occupied by a single object, and the elements with twos are the areas where the two objects overlap. Therefore, a collision takes place if there are elements of the array with the value two.
4. Repeat the above three steps for a given number of times, and count the number of collisions.

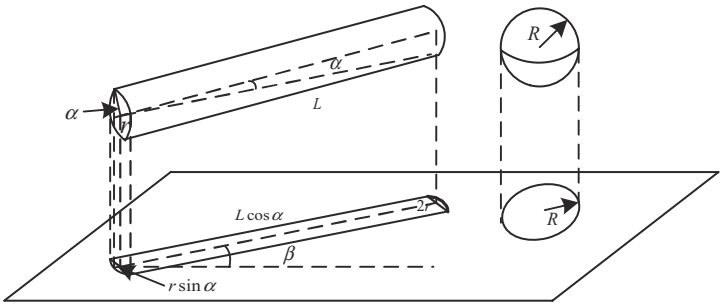


**Figure B-1:** Projection of a sphere and cylinder onto a plane.

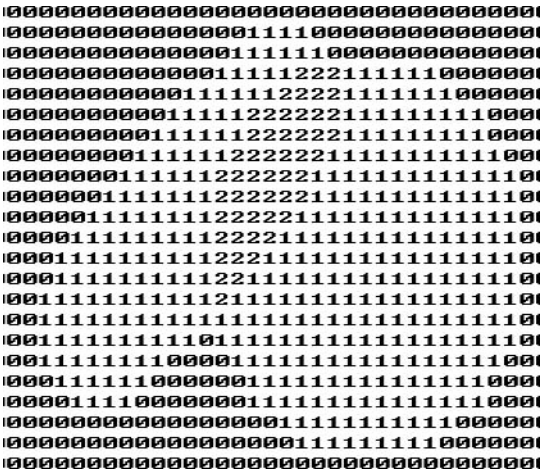

**Figure B-2:** Mapping the projection of a sphere and cylinder on a two-dimension array. This represents only a small part of the two-dimensional field. In the calculation the objects are much smaller than the full.

## B.2 Calculation Results

The objects used in this calculation are a sphere and cylinders with ratios of length to diameter (L/D) of 0.05, 0.2, 1, 3, 5, 10, and 20. All the objects are chosen to have the same total surface area.[4] A cylinder with L/D = 0.05 is a thin disk, which one with L/D = 20 is a long, thin rod.

The two-dimensional array has 10,000 × 10,000 grids, while the surface area of each shape is 2,010,619 grids, which corresponds to a sphere with a radius of 400. The disk with L/D = 0.05 with then have a thickness of 54 and diameter of 1079, while the rod with L/D = 20 will have a length of 3534 and a diameter of 177.

For each pair of objects, the procedure is repeated 20,000 times. The calculation results are listed in Table B-1.

Table B-1 shows that the collision probability between two spheres is the smallest of all the pairs of objects considered. The probability of collision between a sphere and a long rod is nearly 40% larger than between two spheres. The probability of collision between two long rods is more than twice the probability between two spheres.

A "shape coefficient" $\sigma$ is defined by:

$$\sigma = \frac{4A_{cca}}{A_{sf}} \tag{3}$$

where $A_{cca}$ is the actual average collision cross-section area and $A_{sf}$ is the surface area.

**Table B-1:** Collision numbers for different shapes with the same surface area for 20,000 simulations in each case. **The background area is 10,000 × 10,000 grids and the surface area of each shape is 2,010,619 grids.**

| | Sphere | L/D = 0.05 | L/D = 0.2 | L/D = 1 | L/D = 3 | L/D = 5 | L/D = 10 | L/D = 20 |
|---|---|---|---|---|---|---|---|---|
| Sphere | **371** | 408 | 407 | 373 | 390 | 402 | 468 | 512 |
| | L/D = 0.05 | 502 | 459 | 416 | 421 | 459 | 523 | 581 |
| | | L/D = 0.2 | 442 | 405 | 395 | 469 | 507 | 575 |
| | | | L/D = 1 | 368 | 392 | 399 | 469 | 517 |
| | | | | L/D = 3 | 393 | 407 | 484 | 539 |
| | | | | | L/D = 5 | 415 | 517 | 573 |
| | | | | | | L/D = 10 | 583 | 624 |
| | | | | | | | L/D = 20 | 801 |

**Table B-2:** Shape coefficients for the objects used for Table B-1.

| Sphere | L/D = 0.05 | L/D = 0.2 | L/D = 1 | L/D = 3 | L/D = 5 | L/D = 10 | L/D = 20 |
|---|---|---|---|---|---|---|---|
| 1.00 | 1.12 | 1.10 | 1.00 | 1.04 | 1.10 | 1.26 | 1.40 |

For a sphere, $\sigma = 1$. For other objects, the coefficients can be determined by minimizing the function,

$$f = \sum_i \sum_j \left| \sigma_i \sigma_j - N_{i,j}/371 \right| \tag{4}$$

Where $N_{i,j}$ is collision number for object $i, j$, listed in Table B-1.

The calculation results are listed in table B-2. The error of the shape coefficients ($|371\sigma_i\sigma_j - N_{i,j}|/N_{i,j}$) is typically below 2%, which means the coefficient is good enough for converting surface area to effective collision cross sectional area.

The results in Table B-2 indicate that if L/D is close to 1, Kessler's assumption is correct and the impact of shape on collision probability can be neglected. However, when L/D is less than about 0.2 or greater than about 5, the shape influences the collision probability and must be considered. Moreover, since the shape coefficient of a sphere is at the minimum of these objects, using Kessler's approach would underestimate the collision probability of space objects.

Due to gravity stabilization, long thin objects will tend to align pointing toward the center of the Earth, which results in an even larger effective collision cross sectional area. It is interesting to note that the July 1996 collision was between a piece of debris and the Cerise satellite's gravity-gradient stabilization boom.

This analysis shows that the shapes of objects in space can significantly affect their collision probability. For long rods the collision probability could increase by 40% with respect to previous estimates. Because of the importance of estimating collision probabilities between objects in orbit, more research is needed on the effect of more complicated shapes and objects do not have same surface area.

## NOTES AND REFERENCES

1. The z-axis of the coordination system always points from the object along the Earth radius vector toward the Earth's center. The x-axis of the coordination system points in the direction of the velocity vector and is perpendicular to the radius vector. The y-axis is normal to the orbital plane.

2. P. P. Russell, "General Method for Calculating Satellite Collision Probability," Journal of guidance control and dynamics 24 (2001): 716–722.

3. D. J. Kessler and A.-M. P. D., "Critical Number of Spacecraft in Low Earth Orbit: Using Satellite Fragmentation Data to Evaluate the Stability of the Orbital Debris Environment," (paper presented at the Proceedings of the Third European Conference on Space Debris, 2001).

4. This constraint on the objects is used to compare with result to Kessler.